Joint Resource Allocation and Beamforming Design for BD-RIS-Assisted Wireless-Powered Cooperative Mobile Edge Computing

Xintong Qin, Wenjuan Yu, *Member, IEEE*, Qiang Ni, *Senior Member, IEEE*, Zhengyu Song, *Member, IEEE*, Tianwei Hou, *Member, IEEE*, and Xin Sun

***Abstract*—The wireless-powered mobile edge computing (MEC) has emerged as a promising technique to provide energy supplies and computing services for users in Internet of Things (IoT). However, the limited computational resources and poor channel conditions in traditional wireless-powered MEC systems hinder their ability to meet growing user demands. In this paper, we propose a novel beyond-diagonal reconfigurable intelligent surface (BD-RIS) assisted wireless-powered cooperative MEC model to address these challenges. To maximize the total number of completed task bits, we develop a joint resource allocation and beamforming algorithm based on the penalty and Riemannian trust-region methods to jointly optimize the energy transfer time, transmit power, CPU frequencies of users, bandwidth allocation, and the beamforming of BD-RIS. Simulation results demonstrate that the proposed cooperative computing model significantly improves the total number of completed task bits and highlights the superiority of fully-connected BD-RIS over RIS and simultaneous transmission and reflection RIS (STAR-RIS) in wireless-powered MEC systems.**

***Index Terms*—Wireless-powered cooperative MEC, BD-RIS, resource allocation, beamforming design.**

I. Introduction

In recent years, driven by the requirements to extend the battery life of users while simultaneously providing them with enhanced computational capabilities, the wireless-powered cooperative mobile edge computing (MEC) has drawn significant attentions [1]–[3]. However, when the channels between the access point (AP)/cooperative node (CN) and users are blocked, both the efficiency of energy transfer and task offloading will be degraded. Fortunately, the reconfigurable intelligent surface (RIS)/simultaneous transmission and reflection RIS (STAR-RIS), characterized by its ability to reconfigure the wireless propagation environment, can be seamlessly employed in the wireless-powered MEC to improve the efficiency of both energy transfer and task offloading [4]–[8].

Nevertheless, the beamforming matrix of RIS/STAR-RIS is constrained to be diagonal, which heavily limits the potentials of RIS/STAR-RIS [9]. To address this issue, the new concept of beyond diagonal RIS (BD-RIS) is recently proposed. Unlike RIS/STAR-RIS, where each element operates independently,

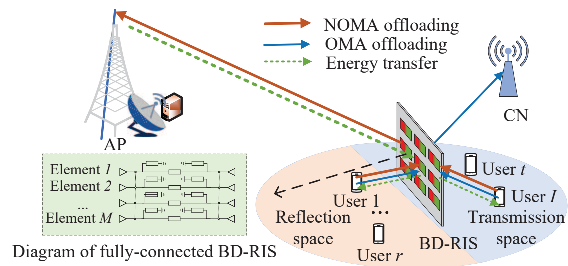

Fig. 1. The BD-RIS-assisted wireless-powered cooperative MEC.

BD-RIS introduces inter-element connections. This fully-connected structure allows BD-RIS to adjust both diagonal and non-diagonal elements of the beamforming matrix, offering greater degrees of freedom (DoFs) for signal propagation manipulation [10]. It has been proved that via inter-element connections, the BD-RIS can further improve the upper bound of the cascaded channel gains compared to traditional RIS. While conceptually promising, the performance gain of fully-connected BD-RIS over single-connected RIS/STAR-RIS in wireless-powered cooperative MEC remains unclear and requires further investigations. Besides, considering the increased dimensionality of the optimization variables and the increased coupling among them, the beamforming design for the BD-RIS is more challenging than that for conventional RIS. A physics-compliant equivalent diagonal representation method for BD-RIS is proposed in [11] that enables the direct application of algorithms developed for conventional RIS to BD-RIS. However, since our study does not focus on the hardware specifics of BD-RIS, we do not leverage this diagonal representation in this letter.

Driven by the above observations, in this paper, we investigate the BD-RIS-assisted wireless-powered cooperative MEC, where the users can simultaneously offload task bits to the AP and CN under the assistance of BD-RIS. A joint resource allocation and beamforming algorithm based on the penalty method and Riemannian trust-region method is proposed to maximize the total number of completed task bits. Simulation results demonstrate the proposed algorithm can further improve the total number of completed task bits, and reveal the superiority of BD-RIS over RIS/STAR-RIS.

II. System Model and Problem Formulation

A. System Model

As shown in Fig. 1, we consider a BD-RIS-assisted wireless-powered cooperative MEC system, where the M-element BD-RIS owns a fully-connected structure and operates in the simultaneous transmission and reflection mode [10]. Define the mission period as T. The beamforming matrices of BD-RIS for transmission and reflection are denoted as

Manuscript received November 4, 2024; revised December 1, 2024 and March 3, 2025; accepted March 14, 2025. Date of publication March 14, 2025; date of current version March 14, 2025. This work was supported by the National Natural Science Foundation of China under Grant 61901027. The associate editor coordinating the review of this article and approving it for publication was Fco. Rafael Lima. *(Corresponding author: Zhengyu Song.)*

X. Qin, Z. Song, T. Hou, and X. Sun are with the School of Electronic and Information Engineering, Beijing Jiaotong University, Beijing 100044, China (e-mails: 20111046@bjtu.edu.cn, songzy@bjtu.edu.cn, twhou@bjtu.edu.cn, xsun@bjtu.edu.cn).

W. Yu and Q. Ni are with the School of Computing and Communications, InfoLab21, Lancaster University, Lancaster LA1 4WA, U.K. (e-mails: w.yu8@lancaster.ac.uk, q.ni@lancaster.ac.uk).

$\mathbf{\Theta}_t^D \in \mathbb{C}^{M\times M}$ and $\mathbf{\Theta}_r^D \in \mathbb{C}^{M\times M}$, respectively [1]. The direct links among the AP and users are assumed to be blocked by obstacles [12]. The downlink channels from AP to the BD-RIS and that from BD-RIS to user $i \in \mathcal{I}$ can be represented as $\mathbf{H}_{\mathrm{AP,RIS}}^D$ and $\mathbf{H}_{\mathrm{RIS},i}^D$, respectively. Similar to [12], the Rician fading channel model is adopted for all channels involved in this paper. Taking the downlink channel from the BD-RIS to user i as an example, we have $\mathbf{H}_{\mathrm{RIS},i}^D = \sqrt{\frac{\varsigma_{\mathrm{RIS},i}}{1+\varsigma_{\mathrm{RIS},i}}}\mathbf{H}_{\mathrm{RIS},i}^{\mathrm{LoS}} + \sqrt{\frac{1}{1+\varsigma_{\mathrm{RIS},i}}}\mathbf{H}_{\mathrm{RIS},i}^{\mathrm{NLoS}}$, where $\varsigma_{\mathrm{RIS},i}$ indicates the Rician factor. $\mathbf{H}_{\mathrm{RIS},i}^{\mathrm{LoS}}$ and $\mathbf{H}_{\mathrm{NRIS},i}^{\mathrm{LoS}}$ are line-of-sight (LoS) and non-LoS (NLoS) components, respectively. The LoS component $\mathbf{H}_{\mathrm{RIS},i}^{\mathrm{LoS}}$ can be given by $\mathbf{H}_{\mathrm{RIS},i}^{\mathrm{LoS}} = L_{\mathrm{RIS},i}\mathbf{e}_{\mathrm{RIS},i}^{\mathrm{A}}\left(\beta_{\mathrm{RIS},i}, \gamma_{\mathrm{RIS},i}\right)$, where $L_{\mathrm{RIS},i}$ represents the distance-dependent path loss between user i and BD-RIS. We have $L_{\mathrm{RIS},i} = \sqrt{L_0 d_{\mathrm{RIS},i}^{-\alpha_{\mathrm{RIS},i}}}$, where L_0 is the path loss at a reference distance of 1m. $d_{\mathrm{RIS},i}$ denotes the distance between the BD-RIS and user i. $\alpha_{\mathrm{RIS},i}$ represents the path loss factor. $\mathbf{e}_{\mathrm{RIS},i}^{\mathrm{A}}\left(\beta_{\mathrm{RIS},i}, \gamma_{\mathrm{RIS},i}\right) = \left\{\exp\left(j\pi\left(m-1\right)\sin\beta_{\mathrm{RIS},i}\sin\gamma_{\mathrm{RIS},i}\right)\right\}_{m=1}^M \in \mathbb{C}^{M\times 1}$ is the receive array steering vectors with the effective angles of arrival (AOAs). $\beta_{\mathrm{RIS},i}$ and $\gamma_{\mathrm{RIS},i}$ represent the azimuth and elevation of AOA. The NLoS component $\mathbf{H}_{\mathrm{RIS},i}^{\mathrm{NLoS}}$ can be expressed as $\mathbf{H}_{\mathrm{RIS},i}^{\mathrm{NLoS}} = L_{\mathrm{RIS},i}\boldsymbol{\eta}_{\mathrm{RIS},i}$, where $\boldsymbol{\eta}_{\mathrm{RIS},i} \sim \mathcal{CN}\left(0, \mathbf{I}_M\right)$. Denote the transmit power of AP and the energy transfer time as P_{AP} and τ. In this paper, we adopt a non-linear energy harvesting model which takes the circuit saturation effects into consideration. The energy power that user i harvest during τ can be expressed as [8]

$$E_i^{\mathrm{har}} = \frac{\upsilon}{\left(1-\chi\right)\left(1+\exp\left(-\psi\left(P_{\mathrm{input},i}-\phi\right)\right)\right)} - \frac{\upsilon\chi}{\left(1-\chi\right)}, \quad (1)$$

where $\chi = 1/(1+\exp\left(\psi\phi\right))$. υ, ψ, and ϕ are constants related to the circuit specifications. $P_{\mathrm{input},i} = P_{\mathrm{AP}}\left|\mathbf{H}_{\mathrm{RIS},i}^D\mathbf{\Theta}_e^D\mathbf{H}_{\mathrm{AP,RIS}}^D\right|^2$, where $e = \{t, r\}$. If user i is located at the refection space, $e = r$; otherwise, $e = t$ [2].

With the harvested energy, users will simultaneously perform local computing and task offloading in the rest of mission period. For local computing, the number of completed task bits and the energy consumption of user i can be expressed as

$$L_i^{\mathrm{loc}} = \frac{f_i\left(T-\tau\right)}{C_i}, \quad E_i^{\mathrm{loc}} = \kappa\left(T-\tau\right)f_i^3, \quad (2)$$

where f_i is the CPU frequency of user i. C_i is the CPU cycles required for processing 1-bit of task-input data, and κ is the capacitance coefficient.

When users perform task offloading, a hybrid NOMA protocol is adopted. Specifically, it is assumed that every two users form a cluster. The two-user NOMA configuration can achieve a balance between spectral efficiency improvement and implementation feasibility, which has been widely adopted in numerous literature. If user i belongs to cluster $k \in \mathcal{K}$, we have $\delta_{i,k} = 1$; otherwise, $\delta_{i,k} = 0$. In this paper, to ensure the convergence of proposed iterative algorithms, we assume that $\delta_{i,k}$ is pre-given. $\delta_{i,k}$ is computed based on their initial channel gains to the AP. Specifically, all users are first ranked in descending order based on their initial channel gains, and then the user with the highest channel gain is successively paired with the user with the lowest channel gain until all users are paired. All users in cluster k can simultaneously offload task bits to the AP via NOMA, with the bandwidth for NOMA in cluster k denoted as B_k^{NOMA}. Given the transmit power of user i to AP as p_i^{NOMA}, user i's offloading data rate via NOMA can be expressed as

$$R_i^{\mathrm{NOMA}} = \sum_{k=1}^{K}\left(T-\tau\right)B_k^{\mathrm{NOMA}}\log\left(1+\frac{\delta_{i,k}p_i^{\mathrm{NOMA}}\mathbf{h}_i^{\mathrm{NOMA}}}{\Gamma_k + B_k^{\mathrm{NOMA}}n_{\mathrm{AP}}^2}\right), \quad (3)$$

where $\mathbf{h}_i^{\mathrm{NOMA}} = \left|\mathbf{H}_{i,\mathrm{RIS}}^U\mathbf{\Theta}_e^U\mathbf{H}_{\mathrm{RIS,AP}}^U\right|^2$ and $\Gamma_k = \sum_{\tilde{i}=1,\tilde{i}\neq i}^I \delta_{\tilde{i},k}p_{\tilde{i}}^{\mathrm{NOMA}}\mathbf{h}_{\tilde{i}}^{\mathrm{NOMA}}$. $\mathbf{H}_{i,\mathrm{RIS}}^U$ and $\mathbf{H}_{\mathrm{RIS,AP}}^U$ are uplink channels from user i to BD-RIS and that from BD-RIS to the AP, respectively. n_{AP}^2 is the variance of the additive white Gaussian noise (AWGN) at the AP. $\mathbf{\Theta}_e^U$ represents the beamforming matrix of BD-RIS for task offloading. By adjusting $\mathbf{\Theta}_e^U$ and $\mathbf{\Theta}_e^D$ in the corresponding phase, we can fully harness the potential of BD-RIS, thereby meeting the distinct requirements of reconfiguring the wireless propagation environment during task offloading and energy transfer.

When user i in cluster k offload task bits to the AP via NOMA, it can simultaneously offload task bits to the CN via OMA under different frequency bands. Denote the allocated OMA bandwidth for user i in cluster k as $B_{i,k}^{\mathrm{OMA}}$. The total bandwidth for OMA in cluster k can be expressed as $B_k^{\mathrm{OMA}} = \sum_{i=1}^I \delta_{i,k}B_{i,k}^{\mathrm{OMA}}$. The offloading data rate of user i to the CN via OMA can be expressed as

$$R_i^{\mathrm{OMA}} = \sum_{k=1}^{K}\left(T-\tau\right)B_{i,k}^{\mathrm{OMA}}\log\left(1+\frac{\delta_{i,k}p_i^{\mathrm{OMA}}\mathbf{h}_i^{\mathrm{OMA}}}{B_k^{\mathrm{OMA}}n_{\mathrm{CN}}^2}\right), \quad (4)$$

where p_i^{OMA} is the transmit power of user i to CN. $\mathbf{h}_i^{\mathrm{OMA}} = \left|\mathbf{H}_{i,\mathrm{RIS}}^U\mathbf{\Theta}_e^U\mathbf{H}_{\mathrm{RIS,CN}}^U\right|^2$, where $\mathbf{H}_{\mathrm{RIS,CN}}^U$ is the channel from BD-RIS to CN. n_{CN}^2 is the variance of AWGN at the CN.

Thus, the total offloading data rate of user i can be expressed as $R_i^{\mathrm{H}} = R_i^{\mathrm{NOMA}} + R_i^{\mathrm{OMA}}$.

B. Problem Formulation

In this paper, we aim to maximize the total number of completed task bits. Accordingly, the optimization problem can be formulated as

$$
\begin{aligned}
\text{(P1)} \quad & \max_{\mathbf{p},\mathbf{f},\mathbf{B},\mathbf{\Psi},\tau} \sum_{i=1}^{I}\left(R_i^{\mathrm{H}} + L_i^{\mathrm{loc}}\right) && \text{(5a)}\\
& \text{s.t. } B_k^{\mathrm{OMA}} + B_k^{\mathrm{NOMA}} \le B_k, \forall k, && \text{(5b)}\\
& \left(T-\tau\right)\left(p_i^{\mathrm{NOMA}} + p_i^{\mathrm{OMA}}\right) + E_i^{\mathrm{loc}} \le E_i^{\mathrm{har}}\tau, \forall i, && \text{(5c)}\\
& \mathbf{\Psi}_{D/U}^H\mathbf{\Psi}_{D/U} = \mathbf{I}_M, && \text{(5d)}\\
& 0 \le \tau \le T, && \text{(5e)}\\
& p_i^{\mathrm{NOMA}} + p_i^{\mathrm{OMA}} \le P_{\max}, \forall i, && \text{(5f)}\\
& 0 \le f_i \le F_{\max}, \forall i, && \text{(5g)}
\end{aligned}
$$

where $\mathbf{p} \triangleq \left\{p_i^{\mathrm{NOMA}}, p_i^{\mathrm{OMA}}\right\}_{i\in\mathcal{I}}$, $\mathbf{f} \triangleq \left\{f_i\right\}_{i\in\mathcal{I}}$, $\mathbf{B} \triangleq \left\{B_{i,k}^{\mathrm{OMA}}, B_k^{\mathrm{NOMA}}\right\}_{i\in\mathcal{I},k\in\mathcal{K}}$, and $\mathbf{\Psi} = \left[\mathbf{\Theta}_t^{D/U}, \mathbf{\Theta}_r^{D/U}\right]^H$. (5b)

[1]The beamforming matrices are sub-matrices of the scattering matrices [12], which can be converted into an impedance matrix for circuit design.

[2]A linear cascaded channel model is adopted in this paper, which ignores the mutual coupling caused by the proximity and multipath propagation [13]. The resource allocation and beamforming design based on more practical channel model, such as the PhysFad [14], will be left as our future work.

represents that the total bandwidth of each cluster is divided into the NOMA bandwidth and OMA bandwidth. (5c) implies that the energy consumption of users must not exceed the energy they have harvested. (5d) is the unique constraint of fully-connected BD-RIS. We do not specify any other mathematical characteristics of $\mathbf{\Theta}_t^D$ and $\mathbf{\Theta}_t^D$. [10]

III. Joint resource allocation and beamforming

Problem (P1) is a non-convex problem since constraint (5d) is a unitary constraint, and the optimization variables are highly coupled with each other. Meanwhile, problem (P1) is also a feasibility-check problem because the downlink beamforming of BD-RIS is independent of the objective function. Therefore, in order to solve such a challenging optimization problem, we propose a joint resource allocation and beamforming algorithm based on the penalty method and the Riemannian trust-region method, where the energy transfer time, transmit power, CPU frequencies, bandwidth allocation and the beamforming of BD-RIS can be iteratively optimized.

Firstly, with given $\mathbf{p}, \mathbf{f}, \mathbf{B}$, and $\mathbf{\Psi}$, we derive the closed-form expression for the optimal energy transfer time. If user i belongs to cluster k, the derivative of the objective function of (P1) with respect to τ can be given by

$$\begin{aligned}\nabla_\tau \left(R_i^{\mathrm{H}}+L_i^{\mathrm{loc}}\right)=&-B_k^{\mathrm{NOMA}}\log(1+\tfrac{\delta_{i,k}p_i^{\mathrm{NOMA}}\mathbf{h}_i^{\mathrm{NOMA}}}{\Gamma_k+B_k^{\mathrm{NOMA}}n_{\mathrm{AP}}^2})\\ &-B_{i,k}^{\mathrm{OMA}}\log\left(1+\tfrac{\delta_{i,k}p_i^{\mathrm{OMA}}\mathbf{h}_i^{\mathrm{OMA}}}{B_k^{\mathrm{OMA}}n_{\mathrm{CN}}^2}\right)-\tfrac{f_i}{C_i}.\end{aligned} \tag{6}$$

It can be found that $\nabla_\tau \left(R_i^{\mathrm{H}}+L_i^{\mathrm{loc}}\right)\leq 0$ always holds, which indicates that the objective function of (P1) is a monotonically decreasing function of τ and the optimal solution to τ can be decided by its lower bound. Thus, considering the constraints (5c) and (5e), the closed-form expression for optimal energy transfer time can be derived as

$$\tau^* = \min\left\{\frac{T\left(p_i^{\mathrm{NOMA}}+p_i^{\mathrm{OMA}}+\kappa f_i^3\right)}{E_i^{\mathrm{har}}+p_i^{\mathrm{NOMA}}+p_i^{\mathrm{OMA}}+\kappa f_i^3}, T\right\}. \tag{7}$$

Then, with obtained τ^*, and given $\mathbf{\Psi}$, (P1) is reformulated as

$$\begin{aligned}&(\mathrm{P2})\ \max_{\mathbf{p},\mathbf{f},\mathbf{B}} \sum_{i=1}^{I}\left(R_i^{\mathrm{H}}+L_i^{\mathrm{loc}}\right)\\ &\mathrm{s.t.}\ (5\mathrm{b}),(5\mathrm{c}),(5\mathrm{f}),(5\mathrm{g}).\end{aligned} \tag{8}$$

Since problem (P2) is a standard convex optimization problem, it can be solved via efficient numerical methods, such as the interior-point method.

Finally, with obtained τ^*, $\mathbf{p}^*$, $\mathbf{f}^*$, and $\mathbf{B}^*$, we focus on the beamforming design for BD-RIS. Since the optimization variable $\mathbf{\Psi}_D$ in constraint (5c) is irrelevant with the objective function (5a), to tackle this problem, the penalty method is utilized to reformulate the objective function, where constraint (5c) is incorporated into the original objective function (5a) as a penalty term. Thus, problem (P1) can be reformulated as

$$\begin{aligned}(\mathrm{P3})\ \max_{\mathbf{\Psi}}&\sum_{i=1}^{I}\left(R_i^{\mathrm{H}}+L_i^{\mathrm{loc}}\right)\\ &+\sum_{i=1}^{I}\mu_i\left(E_i^{\mathrm{har}}\tau-\left((T-\tau)\left(p_i^{\mathrm{NOMA}}+p_i^{\mathrm{OMA}}\right)+E_i^{\mathrm{loc}}\right)\right)\end{aligned} \tag{9a}$$

$$\mathrm{s.t.}\,\mathbf{\Psi}_{D/U}^H\mathbf{\Psi}_{D/U}=\mathbf{I}_M, \tag{9b}$$

where μ_i is the penalty factor. Due to the non-convex objective function (9a) and the unitary constraint (9b), (P3) is still challenging to solve. Fortunately, by leveraging the geometric properties of unitary constraint, the Riemannian trust-region method can avoid the violations of constraint (9b). Meanwhile, compared to the other Riemannian manifold methods, such as the Riemannian Newton's method and Riemannian conjugate gradient method, the Riemannian trust-region method can tackle the non-convex objective function (9a), and ensure the global convergence. Therefore, in this paper, we adopt the Riemannian trust-region method to optimize the the beamforming of BD-RIS. Specifically, constraint (9b) forms a complex Stiefel manifold, i.e.,

$$\mathcal{M}=\left\{\mathbf{\Psi}_{D/U}\in\mathbb{C}^{2M\times M}:\mathbf{\Psi}_{D/U}^H\mathbf{\Psi}_{D/U}=\mathbf{I}_M\right\}. \tag{10}$$

At the l-th iteration, the tangent space of manifold $\mathcal{M}$ can be given by

$$\mathcal{T}_{\mathbf{\Psi}_{D/U}^{(l)}}\mathcal{M}=\left\{\mathbf{T}:\mathcal{R}\left\{\mathbf{\Psi}_{D/U}^{(l)H}\mathbf{T}\right\}=\mathbf{0}_M\right\}. \tag{11}$$

Define the objective function of (P3) as $f(\mathbf{\Psi})$. During the l-th iteration, the trust region subproblem of (P3) can be formulated as

$$\begin{aligned}(\mathrm{P4})\ \max_{\eta\in\mathcal{T}_{\mathbf{\Psi}_{D/U}^{(l)}}\mathcal{M}}\ & m(\eta)=f\left(\mathbf{\Psi}^{(l)}\right)+\left\langle\nabla f\left(\mathbf{\Psi}^{(l)}\right),\eta\right\rangle\\ &+\frac{1}{2}\left\langle\nabla^2 f\left(\mathbf{\Psi}^{(l)}\right)\eta,\eta\right\rangle \end{aligned}\tag{12a}$$

$$\mathrm{s.t.}\ \|\eta\|\leq\Delta^{(l)}, \tag{12b}$$

where Δ represents the radius of trust region. $\left\langle\nabla f\left(\mathbf{\Psi}^{(l)}\right),\eta\right\rangle$ represents the inner product of $\nabla f\left(\mathbf{\Psi}^{(l)}\right)$ and η. Although problem (P4) can be tackled according to the Karush-Kuhn-Tucker (KKT) conditions, the complexity of solving KKT equations will be intolerable when the number of BD-RIS's elements is large. Thus, a Steihaug-Toint truncated conjugate gradient method is adopted to solve (P4), which is summarized as Algorithm 1.

During the t-th iteration of Algorithm 1, there are two conditional statements, which are the negative curvature condition (i.e., $\left\langle\nabla^2 f(\mathbf{\Psi})\,d^{(t)},d^{(t)}\right\rangle<0$) and the trust region boundary condition (i.e., $\left\|\eta^{(t+1)}\right\|\geq\Delta$), respectively. The negative curvature condition prevents the algorithm from proceeding along a descent direction. The trust region boundary condition ensures each iteration's solution remains within the trust region radius. When one of these two conditions is satisfied, we need to update the step length $\lambda^{(t)}$ to ensure the solution of (P4) lies on the boundary of the trust region. Thus, by solving the equation $\left\|\eta^{(t)}+\lambda^{(t)}d^{(t)}\right\|=\Delta$, we can obtain the closed-form expression of $\lambda^{(t)}$ as

$$\lambda^{(t)}=\frac{-\left\langle\eta^{(t)},d^{(t)}\right\rangle+\sqrt{\left\langle\eta^{(t)},d^{(t)}\right\rangle^2-\nu^{(t)}\left\langle d^{(t)},d^{(t)}\right\rangle}}{\left\langle d^{(t)},d^{(t)}\right\rangle}, \tag{13}$$

where $\nu^{(t)}=\Delta^2-\left\langle\eta^{(t)},\eta^{(t)}\right\rangle$. With Algorithm 1, the Riemannian trust-region algorithm for solving (P3) is summarized as Algorithm 2. In Algorithm 2, the trust region radius is updated

Algorithm 1 Steihaug-Toint truncated conjugate gradient method for solving (P4)

Initialize: Set $\eta^{(0)}=0, r^{(0)}=\nabla f\left(\mathbf{\Psi}\right), d^{(0)}=-r^{(0)}$, $t=0$, and $b=0$;
while $\left\|r^{(t)}\right\| > \left\|r^{(0)}\right\| \min\left\{\kappa, \left\|r^{(0)}\right\|^{\varepsilon}\right\}$ **do**
  if $\left\langle \nabla^2 f\left(\mathbf{\Psi}\right) d^{(t)}, d^{(t)}\right\rangle < 0$ **then**
    Calculate $\lambda^{(t)}$ based on (13);
    Set $\eta_b=\eta^{(t)}+\lambda^{(t)}d^{(t)}$ and $b=1$;
    break
  end if
  $\alpha^{(t)}=\langle r^{(t)}, r^{(t)}\rangle / \langle \nabla^2 f(\mathbf{\Theta})d^{(t)}, d^{(t)}\rangle$;
  $\eta^{(t+1)}=\eta^{(t)}+\alpha^{(t)}d^{(t)}$;
  if $\left\|\eta^{(t+1)}\right\| \geq \Delta$ **then**
    Calculate $\lambda^{(t)}$ based on (13);
    $\eta_b=\eta^{(t)}+\lambda d^{(t)}$ and $b=1$;
    break
  end if
  $r^{(t+1)}=r^{(t)}+\alpha^{(t)}\nabla^2 f(\mathbf{\Psi})d^{(t)}$;
  $\beta^{(t+1)}=\langle r^{(t+1)}, r^{(t+1)}\rangle / \langle r^{(t)}, r^{(t)}\rangle$;
  $d^{(t+1)}=-r^{(t+1)}+\beta^{(t+1)}d^{(t)}$;
  $t=t+1$;
end while
$\eta=\eta^{(t)}$;
if $b==1$ **then**
  $\eta=\eta_b$;
end if

Algorithm 2 Riemannian trust-region algorithm for solving problem (P3)

Initialize $\mathbf{\Psi}^{(0)}$, $\Delta^{(0)}$, and set $l=0$;
repeat
  Run Algorithm 1 to obtain $\eta^{(l)}$;
  Calculate $\rho^{(l)}$ and $\Delta^{(l)}$ based on (14) and (15);
  if $\rho^{(l)} > \zeta$ **then**
    $\mathbf{\Psi}^{(l+1)}=Retr_{\mathbf{\Psi}^{(l)}}(\eta^{(l)})$;
  else
    $\mathbf{\Psi}^{(l+1)}=\mathbf{\Psi}^{(l)}$;
  end if
  $l=l+1$;
until the convergence of (P3) or $l>N$

Algorithm 3 Joint resource allocation and beamforming algorithm for BD-RIS-assisted wireless-powered cooperative MEC

Initialize $\mathbf{p}^{(0)}, \mathbf{f}^{(0)}, \mathbf{B}^{(0)}, \mathbf{\Psi}^{(0)}, \tau^{(0)}$, and set $l=0$;
while $\left|\sum_{i=1}^{I}\left(R_i^{\mathrm{H}}+L_i^{\mathrm{loc}}\right)^{(l+1)}-\sum_{i=1}^{I}\left(R_i^{\mathrm{H}}+L_i^{\mathrm{loc}}\right)^{(l)}\right| \geq \varepsilon$ **do**
  Calculate $\tau^{(l)}$ based on (1);
  Solve problem (P2) to obtain $\mathbf{p}^{(l)}, \mathbf{f}^{(l)}$ and $\mathbf{B}^{(l)}$;
  Run Algorithm 2 to obtain $\mathbf{\Psi}^{(l)}$;
  $l=l+1$;
end while

based on $\rho^{(l)}$, which is given by

$$\rho^{(l)}=\frac{f\left(\mathbf{\Psi}^{(l)}\right)-f\left(Retr_{\mathbf{\Psi}^{(l)}}\left(\eta^{(l)}\right)\right)}{m_{\mathbf{\Psi}^{(l)}}\left(0\right)-m_{\mathbf{\Psi}^{(l)}}\left(\eta^{(l)}\right)}, \tag{14}$$

where $Retr\left(\cdot\right)$ is the retraction function. $\rho^{(l)}$ represents the degree of approximation between $m\left(\eta\right)$ and $f\left(\mathbf{\Psi}\right)$. A smaller $\rho^{(l)}$ indicates that the approximation is inadequate. The next iteration cannot sufficiently reduce the objective function, and thus the trust region radius should be reduced. Otherwise, the trust region radius can be increased at the next iteration to accelerate convergence. Define β_1 and β_2 as the coefficients related to the update of trust region radius, with $\beta_1 \in (0,1)$ and $\beta_2 > 1$. The trust region radius at the $(l+1)$-th iteration can be updated as

$$\Delta^{(l+1)}=\begin{cases} \beta_1\Delta^{(l)}, & \text{if } 0<\rho^{(l)}\leq\alpha_1; \\ \Delta^{(l)}, & \text{if } \alpha_1<\rho^{(l)}\leq\alpha_2; \\ \beta_2\Delta^{(l)}, & \text{if } \alpha_2<\rho^{(l)}\leq 1. \end{cases} \tag{15}$$

where α_1 and α_2 are constants, with $0<\alpha_1<\alpha_2<1$.

By executing Algorithm 2, we can obtain the beamforming strategy of BD-RIS. Based on the above solutions to $\tau, \mathbf{p}, \mathbf{f}, \mathbf{B}$, and $\mathbf{\Psi}$, the joint resource allocation and beamforming algorithm for BD-RIS-assisted wireless-powered cooperative MEC is summarized as Algorithm 3, which is in polynomial complexity. In practical implementation, Algorithm 3 is executed at the BS, and then the BS distributes the optimized parameters to users, BD-RIS, and the CN. Besides, since the objective function of problem (P1) is upper-bounded and non-decreasing after each iteration, Algorithm 3 is guaranteed to converge [8].

IV. Simulation Results

In this section, simulation results are provided to evaluate the performance of proposed algorithms. In the simulations, the users are distributed in a circular area with a radius of 2 meters centered at $(10,0,0)$. The AP, CN, and the BD-RIS are located at $(0,3,0)$, $(12,3,0)$, and $(8,0,0)$ respectively. Other simulation parameters are listed in Table I for clarity.

Fig. 2(a) displays the total number of completed task bits versus P_{AP}, where the proposed algorithm is compared with three other schemes. We observe that as P_{AP} increases, the total number of completed task bits also increases for all schemes. This is because users can harvest more energy used for local computing and task offloading when the AP adopts a larger transmit power. It is worth noting that our proposed algorithm can achieve higher total number of completed task bits than STAR-RIS and T-RIS in the wireless-powered cooperative MEC. This is because thanks to the inter-element connections, the BD-RIS can provide more flexibility for channel reconfiguration than STAR-RIS and T-RIS, and thus higher channel gain for both task offloading and energy transfer can be achieved. Besides, we also find that even with the help of BD-RIS, the scheme without CN always exhibits the worst performance, which underscores the advantages of cooperative computing for wireless-powered MEC.

Fig. 2(b) presents the total number of completed task bits versus M. As expected, when M increases, the total number of completed task bits also increases since larger beamforming gain can be achieved by RIS with a larger number of elements. More importantly, in wireless-powered cooperative MEC, the performance gap of BD-RIS over STAR-RIS/T-RIS also widens as M increases. This is because with the

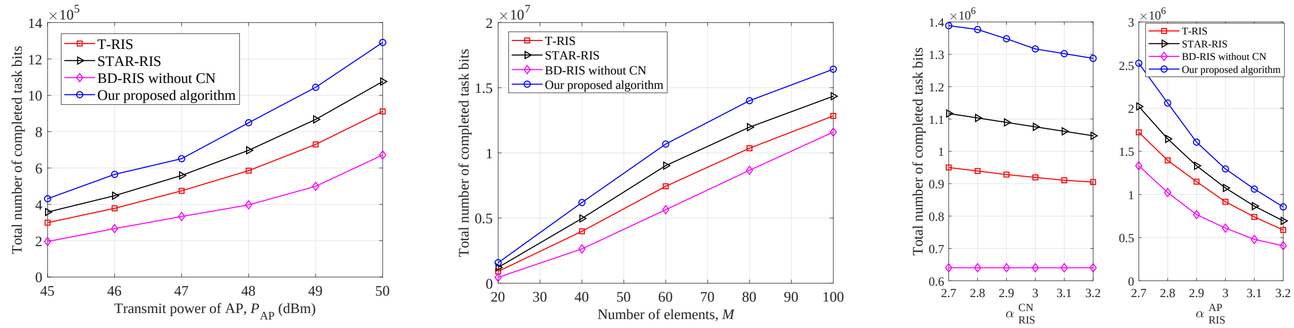

(a) (b) (c)

Fig. 2. (a) The total number of completed task bits versus P_{AP}. (b) The total number of completed task bits versus M. (c) The total number of completed task bits versus $\alpha_{\mathrm{RIS}}^{\mathrm{AP}}$ and $\alpha_{\mathrm{RIS}}^{\mathrm{CN}}$.

TABLE I
SIMULATION PARAMETERS

Parameters	Default Values
Number of users, I	4
Bandwidth, B_k	1 MHz
Noise power, n_{AP}^2, n_{CN}^2	-80 dBm
Rician factor, ς	3 dB
Maximum CPU frequency, $F_{\max}$	1 GHz
Capacitance coefficient, κ	10^{-28}
Energy harvesting parameters, υ, ψ, ϕ	0.0233, 132.8, 0.0118

increase of the number of RIS's elements, the dimension of beamforming matrix expands, and the number of non-diagonal elements which can be adjusted by BD-RIS also increases. Therefore, the performance improvement achieved by BD-RIS becomes more significant compared to STAR-RIS/T-RIS when there are a larger number of RIS's elements.

Fig. 2(c) shows the impacts of path loss factors between RIS and AP/CN on the total number of completed task bits. Besides the scheme of BD-RIS without CN, the performance of all schemes decrease with the increase of $\alpha_{\mathrm{RIS}}^{\mathrm{AP}}$ and $\alpha_{\mathrm{RIS}}^{\mathrm{CN}}$. This is because the channel gains between RIS and AP/CN decrease with the increase of $\alpha_{\mathrm{RIS}}^{\mathrm{AP}}$ and $\alpha_{\mathrm{RIS}}^{\mathrm{CN}}$. Since the users in BD-RIS without CN do not offload task bits to the CN, the total number of completed task bits remains unaffected as $\alpha_{\mathrm{RIS}}^{\mathrm{CN}}$ increases. Moreover, it is observed that the impacts of $\alpha_{\mathrm{RIS}}^{\mathrm{AP}}$ on the total number of completed task bits is significantly greater than that of $\alpha_{\mathrm{RIS}}^{\mathrm{CN}}$. This is because when the channel gains between the AP and RIS degrade, in addition to the decrease of users' offloading data rate, the energy harvested by users also reduces. Additionally, we also find that as $\alpha_{\mathrm{RIS}}^{\mathrm{CN}}$ increases, the performance gain of our proposed algorithm over BD-RIS without CN diminishes. Nevertheless, since the CN is deployed closer to users, the channel gain between users and CN is still higher than that between users and AP even when $\alpha_{\mathrm{RIS}}^{\mathrm{CN}} = 3.2$. Therefore, even with a larger $\alpha_{\mathrm{RIS}}^{\mathrm{CN}}$, our proposed algorithm still performs greatly better than BD-RIS without CN, which demonstrates the necessity to deploy CN for improving the total number of completed task bits in BD-RIS-assisted wireless-powered MEC.

V. CONCLUSIONS

This paper proposed a novel BD-RIS-assisted wireless-powered cooperative MEC to satisfy the increasing computational demands of users. To maximize the total number of completed task bits, an iterative algorithm based on the penalty method and Riemannian trust-region method was proposed to optimize the resource allocation and beamforming design of BD-RIS. Simulation results demonstrated that the BD-RIS outperformed the T-RIS and STAR-RIS in wireless-powered MEC. More importantly, the proposed algorithm can achieve higher total number of completed task bits than the scheme without CN even under a larger path loss factor between BD-RIS and CN, which highlighted the necessity to deploy CN in wireless-powered MEC.

REFERENCES

[1] L. Zhang *et al.*, "Joint terminal pairing and multi-dimensional resource allocation for cooperative computation in a WP-MEC system," *IEEE Trans. Green Commun. Netw.*, vol. 7, no. 3, pp. 1447–1456, Sep. 2023.

[2] Y. Li, X. Zhang *et al.*, "Computation rate maximization for wireless-powered edge computing with multi-user cooperation," *IEEE Open J. Commun. Soc.*, vol. 5, pp. 965–981, 2024.

[3] Y. Zeng *et al.*, "Joint resource allocation and trajectory optimization in UAV-enabled wirelessly powered MEC for large area," *IEEE Internet of Things J.*, vol. 10, no. 17, pp. 15 705–15 722, Sep. 2023.

[4] S. Zhao *et al.*, "Computation offloading and beamforming optimization for energy minimization in wireless-powered IRS-Assisted MEC," *IEEE Internet of Things J.*, vol. 10, no. 22, pp. 19 466–19 478, Nov. 2023.

[5] Y. Li, F. Wang *et al.*, "IRS-Based MEC for Delay-Constrained QoS Over RF-Powered 6G Mobile Wireless Networks," *IEEE Trans. Veh. Technol.*, vol. 72, no. 7, pp. 8722–8737, Jul. 2023.

[6] G. Chen, Q. Wu *et al.*, "IRS-aided wireless powered MEC systems: TDMA or NOMA for computation offloading?" *IEEE Trans. Wireless Commun.*, vol. 22, no. 2, pp. 1201–1218, Feb. 2023.

[7] D.-B. Ha, V.-T. Truong *et al.*, "STAR-RIS-aided UAV NOMA Mobile Edge Computing Network with RF Energy Harvesting," *Mobile Netw Appl*, May 2024.

[8] X. Qin, Z. Song *et al.*, "Joint resource allocation and configuration design for STAR-RIS-enhanced wireless-powered MEC," *IEEE Trans. Commun.*, vol. 71, no. 4, pp. 2381–2395, Apr. 2023.

[9] Z. Guang, Y. Liu *et al.*, "Power minimization for ISAC system using beyond diagonal reconfigurable intelligent surface," *IEEE Trans. Veh. Technol.*, vol. 73, no. 9, pp. 13 950–13 955, Sep. 2024.

[10] H. Li, S. Shen *et al.*, "Reconfigurable intelligent surfaces 2.0: Beyond diagonal phase shift matrices," *IEEE Commun. Mag.*, vol. 62, no. 3, pp. 102–108, Mar. 2024.

[11] P. del Hougne, "A physics-compliant diagonal representation for wireless channels parametrized by beyond-diagonal reconfigurable intelligent surfaces," *arXiv preprint arXiv:2409.20509*, Sep. 2024.

[12] H. Li, S. Shen *et al.*, "Beyond diagonal reconfigurable intelligent surfaces: From transmitting and reflecting modes to single-, group-, and fully-connected architectures," *IEEE Trans. Wireless Commun.*, vol. 22, no. 4, pp. 2311–2324, Apr. 2023.

[13] A. Rabault *et al.*, "On the tacit linearity assumption in common cascaded models of RIS-parametrized wireless channels," *IEEE Trans. Wireless Commun.*, vol. 23, no. 8, pp. 10 001–10 014, Aug. 2024.

[14] R. Faqiri *et al.*, "Physfad: Physics-based end-to-end channel modeling of RIS-parametrized environments with adjustable fading," *IEEE Trans. Wireless Commun.*, vol. 22, no. 1, pp. 580–595, Jan. 2023.